

MULTI-SCALE INTERACTIONS IN A TROPICAL-BELT EXPERIMENT USING THE WRF MODEL



Ricardo FONSECA^{1,2}, Tieh-Yong KOH^{3,1}, Chee-Kiat TEO^{4,5}, Tengfei ZHANG¹

¹Earth Observatory of Singapore, Nanyang Technological University, Singapore

²Khalifa University of Science and Technology, Abu Dhabi, United Arab Emirates

³Centre for University Core, Singapore University of Social Sciences, Singapore

⁴Centre for Climate Research Singapore, Meteorological Service Singapore, Singapore

⁵School of Physical and Mathematical Sciences, Nanyang Technological University, Singapore

(Questions related to sharing of data and/or WRF codes should be directed to tykoh@suss.edu.sg)



SUSSE
SINGAPORE UNIVERSITY OF SOCIAL SCIENCES

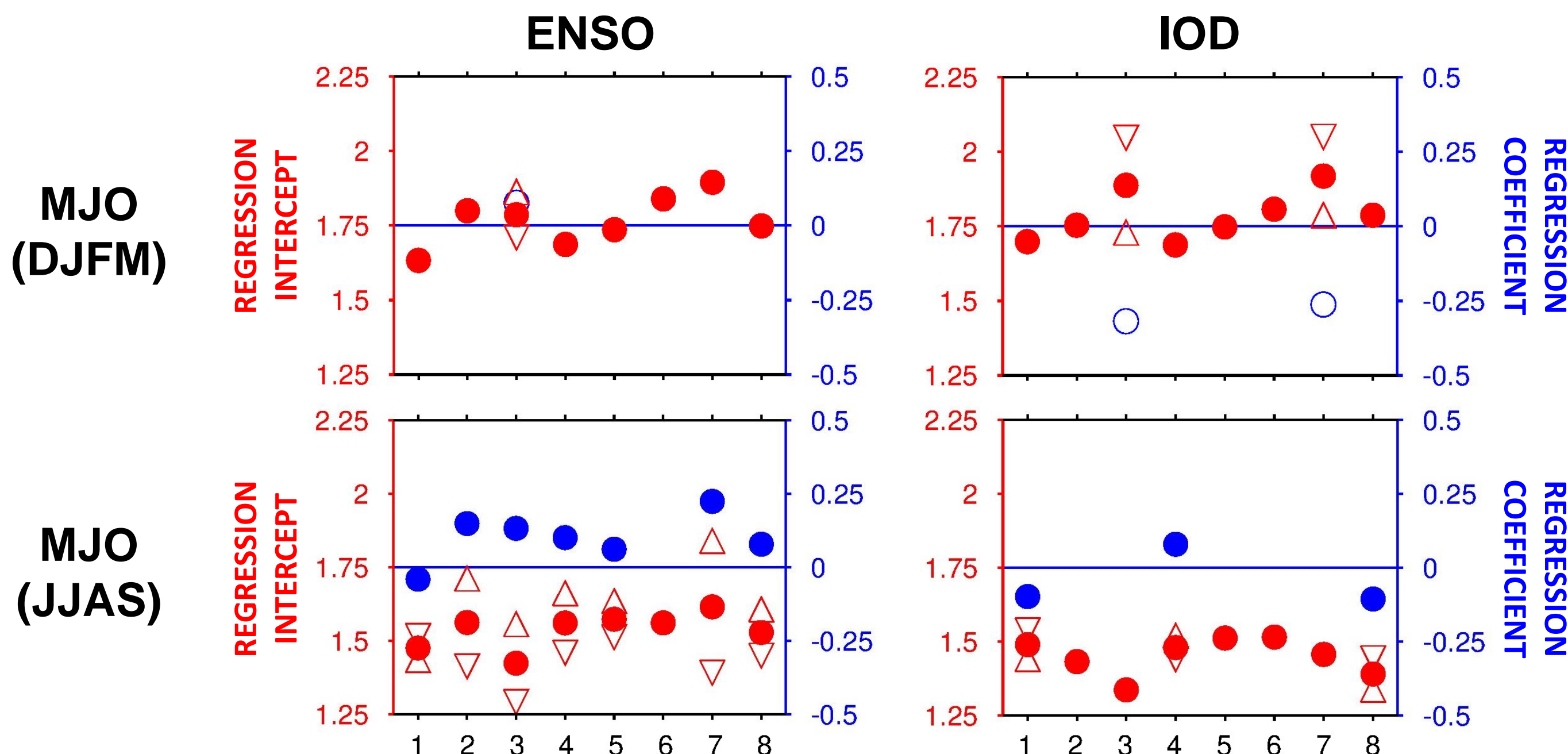


1. Introduction

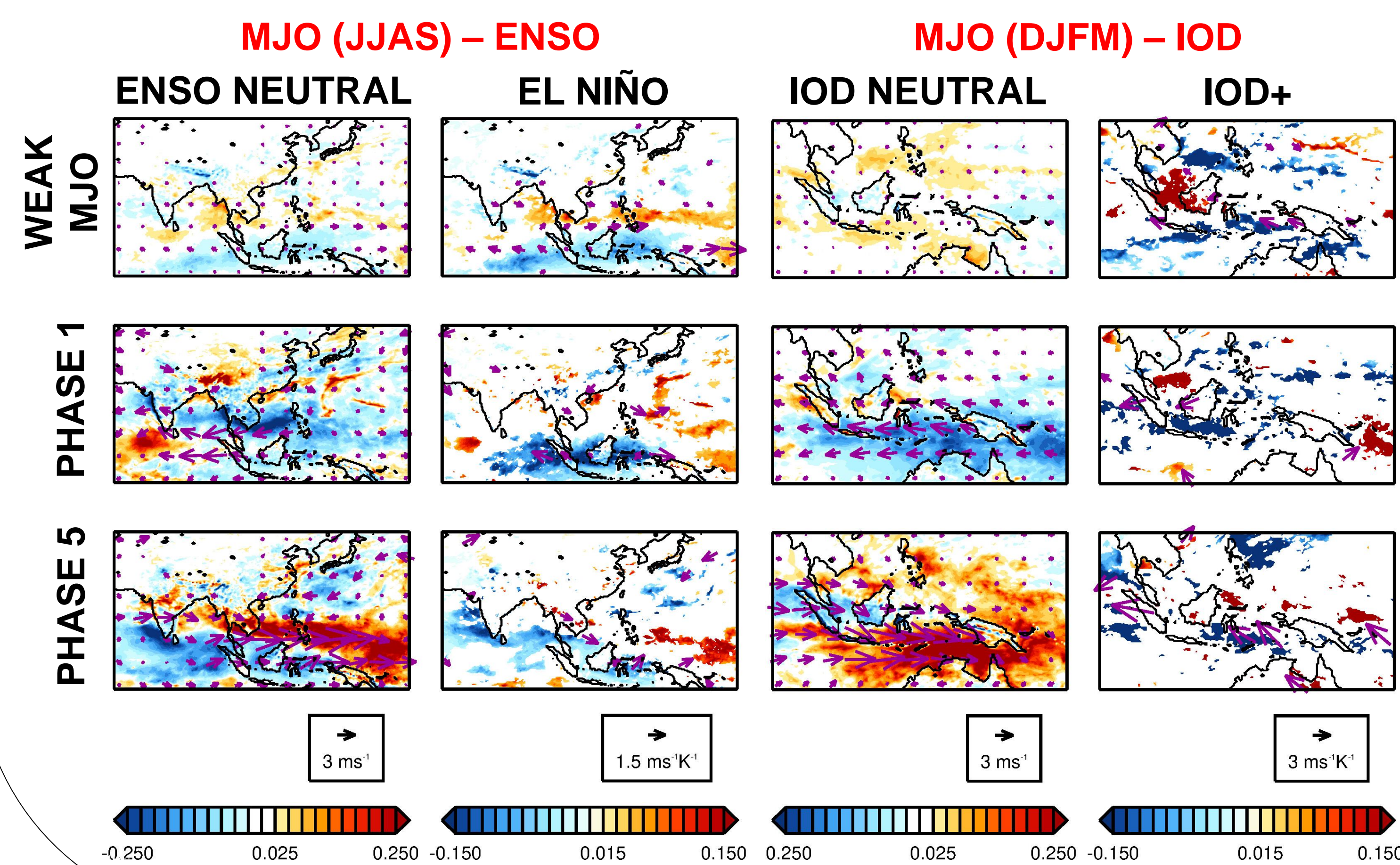
- The Maritime Continent, which consists of the Malay Peninsula, the Philippines, the Greater and Lesser Sunda Islands and New Guinea, comprises small land masses with elevated terrain and shallow seas with the warmest surface temperatures in the world. Coarse resolution General Circulation Models (GCMs) do not capture the geographic variation within the region and so regional climate models are needed to investigate local and regional circulations.
- Given the Maritime Continent's role on the global climate (e.g. Ramage, 1968), an understanding of its regional climate, especially rainfall under intra-seasonal variations, is crucial to establish a baseline for monitoring climate change impacts in Southeast Asia and on the teleconnections elsewhere.

4. MJO – IAV Interactions

- For each phase of the Madden-Julian Oscillation (MJO; Wheeler and Hendon, 2004), and for DJFM and JJAS, we regressed the amplitude of the Real-time Multivariate MJO index (RMM) against the daily ENSO and IOD indices. Below the regression intercept and coefficient (the latter is only plotted if statistically significant at the 90% confidence interval) are shown. The upward (downward) triangles are the MJO amplitude for an anomaly of +1K (-1K) for ENSO and +0.5K (-0.5K) for IOD. The blue circles are only filled if the regression coefficients are statistically significant for 3 or more MJO phases, as in these cases the cross-phase influence of the IAV has a pattern significance of greater than the 90% confidence level.
- The regression intercepts are larger in DJFM compared to JJAS implying stronger MJOs in the former during years neutral to ENSO and IOD, a result consistent with observations (Zhang and Dong, 2004). The impact of El Niño on the MJO amplitude is generally positive in JJAS but practically absent in DJFM. Compared to ENSO, the interaction with IOD is less significant and is also phase dependent.



- Figures below show regression intercept (odd columns from left) and coefficient (even columns from left) of grid-point anomalies of daily mean precipitation rate (units of mm h^{-1} and $\text{mm h}^{-1} \text{K}^{-1}$, respectively) and 850h Pa horizontal wind (m s^{-1} and $\text{m s}^{-1} \text{K}^{-1}$) from the daily climatology for weak MJO events (i.e. MJO amplitude less than 1) and MJO phases 1 and 5 against the daily ENSO index for JJAS and IOD index for DJFM. Only regression coefficients that are statistically significant at the 95% confidence level are plotted. The regression intercepts show WRF capturing well the MJO's regional impacts.
- The regression coefficients for the MJO – ENSO regression resemble the impact of ENSO on the seasonal mean climate, showing that ENSO impacts persist throughout most of the life-cycle of MJO. **Comparing the regression intercept with the regression coefficients, dry regions become drier and wet regions become wetter, implying larger MJO amplitude.** This regional result is consistent with the earlier finding that El Niño is generally associated with an increase of the global MJO amplitude during JJAS. **In DJFM there is a weakening of the MJO impacts in the Maritime Continent in El Niño events** (not shown).
- The impact of IOD on the boreal winter MJO shows the characteristic inter-annual pattern of IOD on the seasonal mean climate. **The impacts of positive IOD events are somewhat mixed, but tend to locally weaken the MJO impacts in the Maritime Continent, despite not necessarily having a significant influence on the global MJO amplitude.** Positive IOD events tend to cause the boreal summer MJO to intensify over the Maritime Continent (not shown).



References

- Andrews, D.G. and Coauthors, 1987: Middle Atmosphere Dynamics. Academic Press, 489 pp.
- Fischer, A. S. and Coauthors, 2005: Two Independent Triggers for the Indian Ocean Dipole/Zonal Mode in a Coupled GCM. *J. Climate*, **18**, 3428–3449.
- Fonseca, R.M. and Coauthors, 2015: Improved Simulation of Precipitation in the Tropics using a Modified BMJ Scheme in WRF Model. *Geosci. Model Dev.*, **8**, 2915–2928.
- Huffman, G.J. and Coauthors, 2007: The TRMM multisatellite precipitation analysis (TMPA): Quasi-global, multiyear, combined-sensor precipitation at fine scales. *J. Hydrometeorol.*, **8**, 38–55.
- Koh, T.-Y. and R.M. Fonseca, 2016: Subgrid-scale Cloud-Radiation Feedback For the Betts-Miller-Janjić Convection Scheme. *Q. J. R. Meteorol. Soc.*, **142**, 989–1006.
- Lestari, R.K. and T.-Y. Koh, 2016: Statistical Evidence for Asymmetry in ENSO-IOD Interactions. *Atmos.-Ocean*, **54**, 498–504.
- Ramage, C.S., 1968: The role of a tropical "maritime continent" in the atmospheric circulation. *Mon. Wea. Rev.*, **96**, 365–370.
- Riciardulli, L. and Coauthors, 2011: Remote Sensing Systems QuickSCAT Ku-2011 Monthly Ocean Wind Vector Winds on 0.25° grid, Version 4. Available at www.remss.com/missions/qscat.
- Saha, S. and Coauthors, 2010: The NCEP Climate Forecast System Reanalysis. *Bull. Amer. Meteor. Soc.*, **91**, 1015–1057.
- Skamarock, W. C. and Coauthors, 2008: A description of the Advanced Research WRF version 3. NCAR tech. note TN-475, STR, 113pp.
- Wheeler, M.C. and H.H. Hendon, 2004: An all-season real-time multivariate MJO index: Development of an index for monitoring and prediction. *Mon. Wea. Rev.*, **132**, 1917–1932.
- Zeng, X. and Beljaars, A., 2005: A prognostic scheme of sea surface skin temperature for modeling and data assimilation. *Geophys. Res. Lett.*, **32**, L14605, doi:10.1029/2005GL023030.
- Zhang, C. and M. Dong, 2004: Seasonality in the Madden-Julian Oscillation. *J. Climate*, **17**, 3160–3180.

2. Regional Atmospheric Climate Model

In this study, the Weather Research and Forecasting model version 3.3.1 (WRF; Skamarok et al., 2008) is used to dynamically downscale 27 years (April 1988 – March 2015) of the $0.5^\circ \times 0.5^\circ$ Climate Forecast System Reanalysis (CFSR; Saha et al., 2010) for the wider tropics.

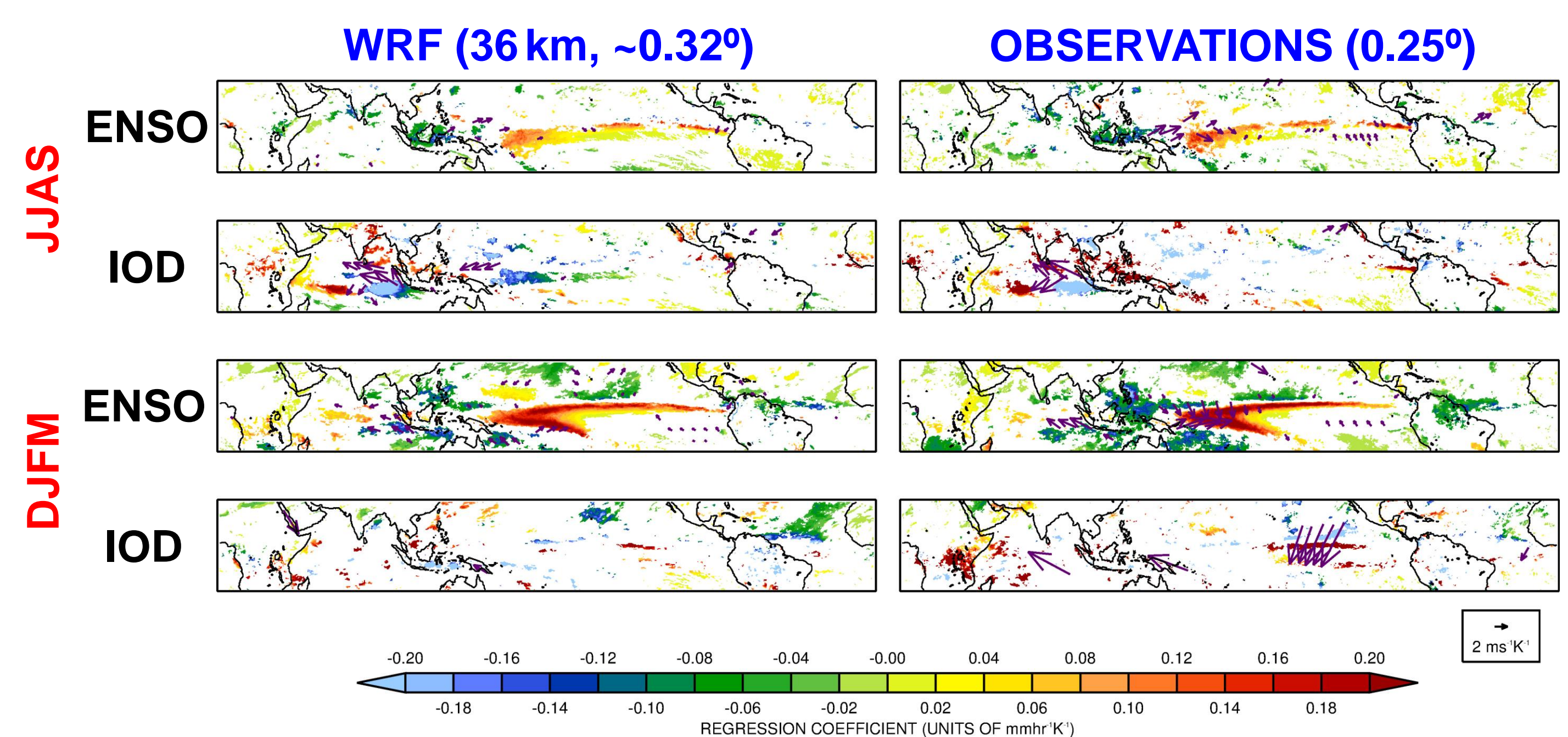
The spatial domain is a tropical belt extending from -36°S to 46°N with a horizontal resolution of 36 km. In all model runs 37 vertical levels are considered, more closely spaced in the Planetary Boundary Layer (PBL) and tropopause region, with the model top at 30 hPa and the highest undamped layer at about 70 hPa. Analysis (grid) nudging is applied to the water vapour mixing ratio (q_v) in the mid-troposphere, while the horizontal winds (u, v) and potential temperature perturbation (θ') are nudged in the lower stratosphere on a time-scale of 1h. The q_v nudging is needed to correct WRF's tendency to overly moisten the atmosphere, while the latter is required for WRF to capture the Quasi-Biennial Oscillation (QBO; Andrews et al., 1987).

The physics parameterization schemes used are shown in the table below:

Physics Options	Parameterization Scheme
Microphysics	Goddard (six-class) Cloud Microphysics Scheme
Radiation	Rapid Radiative Transfer Model for GCM Applications (RRTMG)
Surface Layer	MM5 Monin-Obukhov Scheme
Land Surface	Noah Land Surface Model
Planetary Boundary Layer	Yonsei University (YSU) PBL Scheme
Cumulus	(Modified) Betts-Miller-Janjić (BMJ) Scheme (Fonseca et al., 2015) & Precipitating Convective Cloud (PCC) Scheme (Koh et al., 2016)
Sea Surface Temperature	CFSR SSTs + sea surface skin temperature scheme (Zeng et al., 2005)

3. Inter-Annual Variations (IAV)

- Figures below show regression coefficient of the monthly mean precipitation rate (shading; $\text{mm h}^{-1} \text{K}^{-1}$) and 10-meter horizontal wind (arrows; $\text{m s}^{-1} \text{K}^{-1}$) against the El Niño Southern Oscillation (ENSO) and Indian Ocean Dipole (IOD) indices (Lestari and Koh, 2016) for the boreal summer (June to September, JJAS) and winter (December to March, DJFM) monsoon seasons. The WRF and observed regression coefficients are shown for global tropics (20°S – 30°N), computed over the overlapping period December 1999 – September 2009, and only plotted if statistically significant at 90% confidence interval. For observations, Tropical Rainfall Measuring Mission (TRMM; Huffman et al., 2007) data is used for precipitation and QuickSCAT (Riciardulli et al., 2011) data for the horizontal winds, both at $0.25^\circ \times 0.25^\circ$ spatial resolution.
- WRF is generally capable of capturing observed regression coefficients for both seasons and indices. The IOD impacts are more localized than those of ENSO, confined mainly to the southwest of Sumatra and eastern Indian Ocean where there is a decrease in precipitation in IOD+ events. Drying of Southeast Asia in El Niño events is present in both WRF and observations.



- El Niño events are known to co-occur with IOD+ events and La Niña events with IOD- events (Fischer et al., 2005). In order to assess the importance of the "unusual" co-occurrence of El Niño with IOD- and La Niña with IOD+, two combined indices are defined:

$$EI1 = ENSO \times |IOD|$$

$$EI2 = |ENSO| \times IOD$$

For usual ENSO-IOD co-occurrences, both EI1 and EI2 give the same positive (El Niño with IOD+) or negative (La Niña with IOD-) value so the difference (EI1-EI2) is identically zero. (EI1-EI2) is non-zero only in the "unusual" co-occurrence events: **El Niño with IOD-, La Niña with IOD+.**

- Figures below show regression coefficients against the index (EI1-EI2). A comparison with figure above reveals that **ENSO impacts manifest themselves nearly everywhere in the global tropics in both WRF and observations during the "unusual" co-occurrences of ENSO and IOD.**

- It is important to highlight that even though the amplitude of the regression coefficients against (EI1-EI2) is generally comparable to, or larger than, that obtained in the regression against the separate ENSO and IOD indices, the amplitude of (EI1-EI2) is generally smaller, typically less than 0.5, meaning that the overall impact of the "unusual" co-occurrences of ENSO and IOD will not be as large.

